Acc. Chem. Res. **2001,** *34,* 421−432

Electronically Transduced Molecular Mechanical and Information Functions on Surfaces†

ANDREW N. SHIPWAY AND ITAMAR WILLNER*

Institute of Chemistry and The Farkas Center for Light-Induced Processes, The Hebrew University of Jerusalem, Jerusalem 91904, Israel

Received November 20, 2000

ABSTRACT

Supramolecular chemistry and nanotechnology, along with their use in the construction of functional assemblies and devices, have merged into a challenging field of study. The development of methodologies for the integration and interfacing of molecular building blocks with solid supports and electronic transducers is essential for this research. We address recent applications of molecular, macromolecular, and biomolecular substances in the organization of signal-activated, electronically transduced molecular architectures on electrode surfaces. Photonic, electronic, magnetic, and chemical stimuli are used to trigger the switchable functions of these systems, which demonstrate either mechanical (e.g., translocation) or computational (e.g., memory) functions and provide enlightening insight and directions for the future evolution of the field.

1. Introduction

The pursuit of "bottom-up" nanoscopic solutions to problems of miniaturization and to the advancement of computing, engineering, and medicine is gathering great interest as classical electronics approaches its size limit and the public clamors for ever faster, cheaper, and more efficient devices. The emergence of this multidisciplinary field owes thanks to the relatively recent development of technologies such as supramolecular chemistry,[1] scanning probe microscopies,[2] and surface spectroscopic techniques,[3] which allow the design, characterization, and manipulation of new devices. Broadly speaking, researchers are interested in three different paradigms of function: information functions, mechanical functions, and electronic functions. For the realization of nanotechnologists' dreams, it will be necessary not only to develop units in each of these areas, but also to integrate them into highly functional devices.

Scheme 1. Schematic Representation of an Electrode-Immobilized Optoelectronic Molecule for the Electronic Transduction of Optical Stimuli

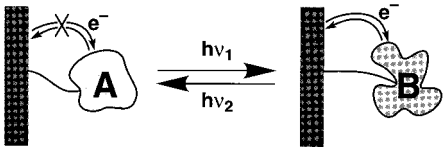

Building blocks for molecular devices are diverse in nature, ranging from well-known photochromic molecules[4] and exotic supramolecular systems[1,5] to biological materials[6] and nanoparticles.[7] These units offer numerous functions such as information storage and processing, sensing, signal transduction and amplification, binding, and catalysis. Mechanical functions such as translocations, rotations, and swelling are of particular interest, as they may offer extremely robust information storage, controllable catalysis, and the interfacing of solid supports with their macroscopic environment. In this Account, we will address the construction of molecular assemblies on electrode surfaces that perform signal-triggered mechanical or information functions. We will discuss the use of light, electrical, magnetic, and chemical stimuli for the activation of these functions and will highlight the electronic transduction of signal-activated events.

2. Molecular Optoelectronic Surfaces

Molecules that are reversibly photoisomerizable between redox-active and redox-inactive states are promising units for the construction of optoelectronic memory devices. The immobilization of these molecules on electrode surfaces allows the optical control (by photoisomerization) of the electronic function (redox activity) of the interface and the electronic transduction of the photonic information (Scheme 1). The assembly of the phenoxynaphthacene quinone **1** on an electrode (Figure 1A) is an excellent example of the construction of such a system. The "*trans*" (**1a**) and "*ana*" (**1b**) states of the molecule are readily interconvertable by irradiation at appropriate wavelengths, and while the *trans* state is electrochemically active ($E^\circ = -0.62$ V vs SCE), the *ana* state is inactive in this potential range.[8] Figure 1A shows how a phenoxynaphthacene quinone monolayer was assembled on a Au electrode by the coupling of 6-[((4-carboxymethyl)phenyl)oxy]-5,12-naphthacene quinone to a self-assembled cystamine monolayer.[9] The cyclic voltammogram of the resulting monolayer shows an ill-defined redox wave for **1a** (Figure 1B, curve a) since a non-densely packed monolayer of

Itamar Willner was born in 1947. He completed his Ph.D. studies in chemistry in 1978 at The Hebrew University of Jerusalem. After a postdoctoral stay with M. Calvin at the University of California, Berkeley, from 1978 to 1981, he joined the Institute of Chemistry at the Hebrew University of Jerusalem in 1981. In 1986, he was appointed as Professor at the Hebrew University. He is a fellow of the American Association for the Advancement of Science (AAAS), serves as a member of several editorial boards, and is the recipient of the Kolthoff Award and the Max-Planck Research Award. His research interests include light-induced electron-transfer processes and artificial photosynthesis, molecular electronics and optoelectronics, bioelectronics and biosensors, optobioelectronics, supramolecular chemistry, nanoscale chemistry, and monolayer and thin-film assemblies.

Andy Shipway was born in 1971 in Bristol, UK. He studied for his B.Sc. at the University of Birmingham and stayed on as a Ph.D. student under the supervision of Prof. J. Fraser Stoddart with a thesis entitled "Insight into Dendrimers and their Role in Catalysis". He joined the group of I. Willner at the Hebrew University in late 1997 as a postdoctoral fellow, coordinating projects involving organic synthesis and nanoparticle superstructures.

† Part of the Special Issue on Molecular Machines.

* To whom correspondence should be addressed. Tel.: 972-2-6585272. Fax: 972-2-6527715. E-mail: willnea@vms.huji.ac.il.

10.1021/ar000180h CCC: $20.00
Published on Web 05/10/2001

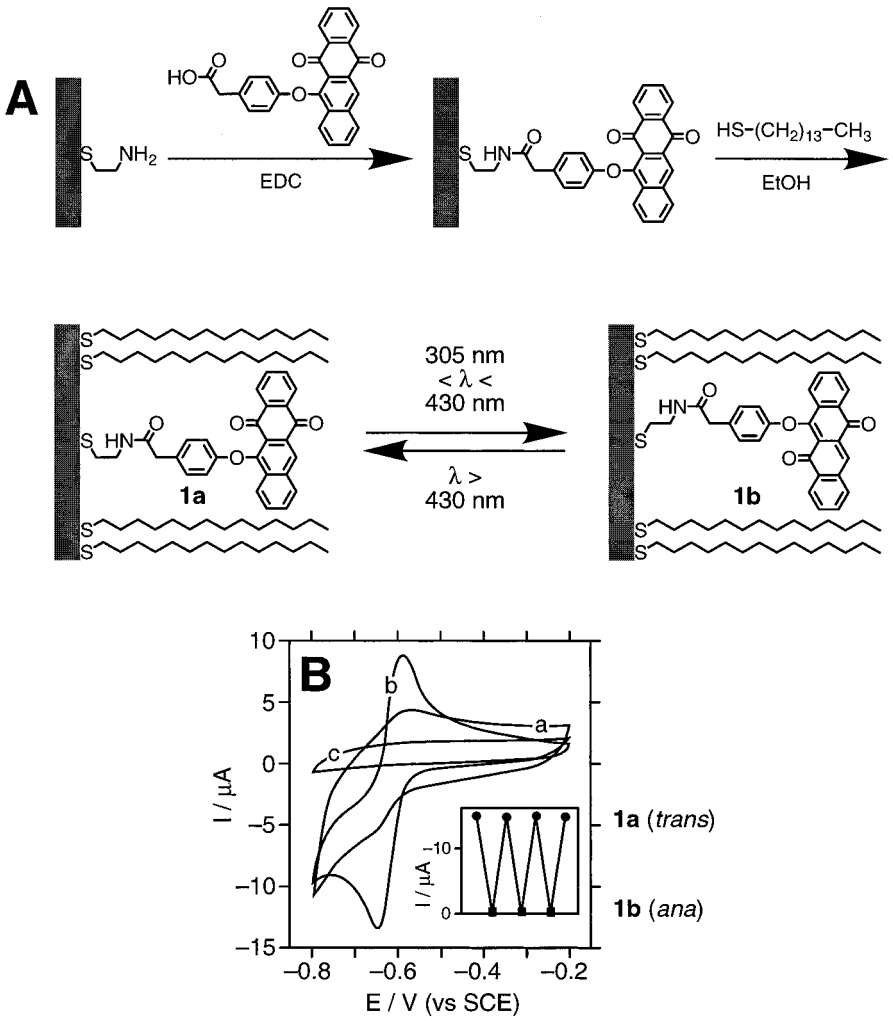

FIGURE 1. (A) Assembly of a phenoxynaphthacene quinone/tetradecanethiol mixed monolayer on a Au electrode and its photoisomerization (EDC = 1-[3-(dimethylamino)propyl]-3-ethylcarbodiimide. (B) Cyclic voltammograms of the *trans*-quinone monolayer (**1a**) (a) before rigidification with tetradecanethiol, (b) after rigidification with tetradecanethiol, and (c) after photoisomerization to the *ana*-quinone state. Inset: Switching of the cathodic peak current upon reversible photoisomerization.

randomly orientated and non-specifically adsorbed molecules is produced. Treatment of the **1a**-functionalized electrode with tetradecanethiol ($C_{14}H_{29}SH$) results in the "stiffening" of the structure, after which the electrode displays a quasi-reversible redox wave (Figure 1B, curve b). After photoisomerization to the **1b** state, only the background current of the electrolyte is observed (Figure 1B, curve c), implying that this photoisomer is redox-inactive within this potential range. By the cyclic photoisomerization of the monolayer between the **1a** and **1b** states, the transduced current is switched reversibly and reproducibly between redox-active and -inactive states (Figure 1B, inset).

Amplification of the electrochemical response can be accomplished by coupling the responsive component to an electron-transfer cascade. In this way, the isomerization of a single molecule leads to a massive signal by "opening the flood gates" to an electrochemical process. The mixed monolayer shown in Figure 2A (consisting of $C_{14}H_{29}SH$ and the **1a**) provides an insulating layer, so electron transfer from the electrode to a solution-state electron relay can take place only when **1** is used as an intermediate relay. In the electrochemically active *trans* (**1a)** state, electron transfer from the redox-active unit to the diffusional relay is possible, so the reduction of the solubilized species proceeds. If the redox unit is isomerized to the *ana* (**1b**) state, it is no longer redox-active, so this electron-transfer cascade is blocked and no electrochemical signal can be generated. This amplification of the electrochemical response to photonic signals can be exemplified by the application of *N*,*N*′-dibenzyl-4,4′-bipyridinium (BV^{2+}, **2**) as the electron relay. The reduction potential of BV^{2+} is $E° = -0.58$ V vs SCE, while the formal reduction potential of **1a** at pH = 7.5 is $E° = -0.65$ V vs SCE. The potential difference between the redox units allows the vectorial reduction of BV^{2+} by the electroactive **1a** monolayer, and thus the activation of an electron-transfer cascade. The transduced current is ca. 10-fold enhanced in the presence of the electron relay. Figure 2B shows the cyclic voltammograms of the photoisomerizable electrode in the **1a** state (curve a) and the **1b** state (curve b) in the presence of BV^{2+}. While the electrocatalytic current is present with the electrode in the **1a** state, photoisomerization of the monolayer to the **1b** state results in only the background

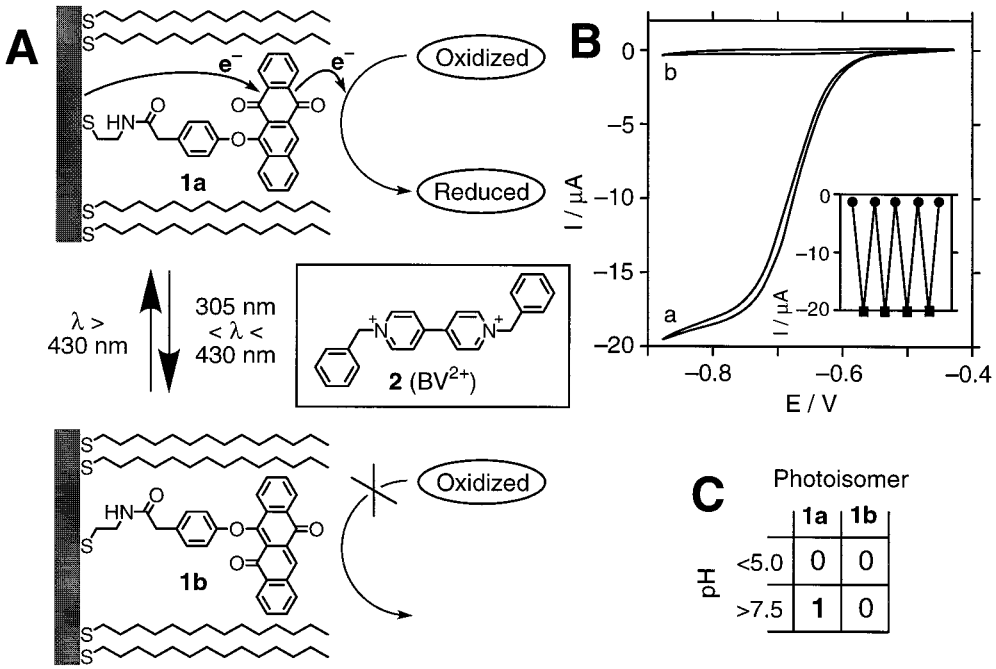

FIGURE 2. (A) Use of dibenzyl viologen (**2**) to amplify the electrochemical signal of the mixed monolayer. (B) Cyclic voltammograms of the electrode in the presence of dibenzyl viologen (1 mM) (a) in the *trans*-quinone state and (b) in the *ana*-quinone state. (C) "AND" behavior of the **1** monolayer.

current (curve b), demonstrating that direct electron transfer to BV^{2+} is prohibited.

The reduction potential of the **1a** monolayer is controlled by the pH of the electrolyte solution and is positively shifted as the pH decreases ($E° = -0.65$ V vs SCE at pH = 7.5 and $E° = -0.51$ V vs SCE at pH = 5.0), while the reduction potential of **2** is pH-independent. The pH-induced shift of the reduction potential of **1a** provides an additional means for controlling the interfacial electron-transfer features at the electrode surface. At pH = 5.0, the **1a** monolayer is thermodynamically prohibited from stimulating electron transfer to BV^{2+} ($E° = -0.58$ V vs SCE). Only a weak electrical response is observed for the **1a** monolayer, without the activation of the electron-transfer cascade. Thus, the phenoxynaphthacene quinone-functionalized monolayer electrode in the presence of BV^{2+} can be described as an "AND" gate with optical and pH inputs that act cooperatively in the activation of an electrochemical output (Figure 2C). The monolayer must be in the **1a** (SP) state "AND" at pH > 7.5 in order to enable vectorial electron transfer and the reduction of BV^{2+}.

Other redox-activated photoisomerizable molecules such as azobenzene[10] and diarylethene[11] have also been immobilized as monolayers on electrode surfaces for optoelectronic applications. An immobilized azobenzene derivative has even been used to perform a "lockable" information storage.[12] A monolayer of 4-octyl-4′-(5-carboxy-pentamethylene-oxy)-*trans*-azobenzene was deposited onto a SnO_2 electrode using the Langmuir−Blodgett method. The monolayer could be reversibly photoisomerized between the *trans* and *cis* states, which revealed differing electrochemical properties. While the *cis*-isomer was readily reduced to the non-photochemically active hydrazobenzene form, the *trans*-isomer was electrochemically inactive in the studied potential range. The reduced state therefore constitutes a "locked" form of the optically written information. The electrochemical oxidation of the hydrazobenzene returned the monolayer selectively into the thermodynamically favored *trans*-isomer, demonstrating an "erase" function.

A different optoelectronic effect can be brought about by a disturbance in a close-packed monolayer upon photoisomerization.[13] The two different isomeric states of an azobenzene monolayer have different packing arrangements, and hence yield different electron-transfer kinetics between the electrode and a solution-state redox probe. Finally, immobilized modified enzymes have been utilized as optoelectronic devices. The tethering of photoisomerizable groups to redox enzymes (e.g., linking nitrospiropyran to glucose oxidase), or the reconstitution of apoenzymes with a photoisomerizable cofactor (e.g., apoglucose oxidase with nitrospiropyran-FAD), yields photoswitchable biocatalysts which can be assembled on electrodes to give photoswitchable bioelectrocatalytic interfaces.[14]

3. "Photocommand" Surfaces

A "photocommand" surface might be defined as a photoisomerizable interface whose different states interact differently with a solution-state species (Scheme 2). This difference allows the controllable association and dissociation of a redox species to and from an electrode, respectively, and thus optical control over its interfacial electron-transfer features. A similar effect can also be obtained from an innate surface which binds one state of a photoisomerizable redox-active solute.[15] It is well known

Scheme 2. Schematic Representation of a "Photocommand Surface" [a]

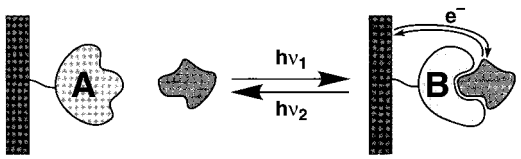

[a] The electrical response of the surface to an external species is controlled by the photoisomeric state of the interface.

that charged interfaces can affect electron-transfer kinetics between an electrode and a charged solution-state species through electrostatic interactions.[16] Negatively charged monolayers associated with electrodes have been shown to discriminate between the electrochemical reactions of a mixture of positively and negatively charged substrates.[17] It is therefore possible to construct a command interface from an isomerizable unit whose states differ in charge. In one example, a nitrospiropyran derivative was assembled on a Au electrode (Figure 3A).[18] While the nitrospiropyran monolayer (**3a**) is neutral, photoisomerization of the monolayer (at pH = 7.0) yields a cationic protonated nitromerocyanine monolayer (**3b**). Oxidation of the negatively charged substrate 3,4-dihydroxyphenyl acetic acid (**4**) and the positively charged 3-hydroxytyramine (dopamine, **5**) was examined at pH = 7.0. Figure 3B (curves a and b) shows the cyclic voltammograms corresponding to the electrochemical oxidation of **4** by the **3a**- and **3b**-state systems. Photoisomerization between the **3a** and **3b** states allows the amperometric response of the electrode to be cycled between low and high values (Figure 3B, inset). With the positively charged electroactive substrate **5**, the direction of the transduced amperometric signals is reversed. Figure 3C shows the cyclic voltammograms of **5** in the presence of **3a** and **3b** electrodes (curves a and b), and the inset shows the reversible cycling of the amperometric response.

A nitrospiropyran/protonated nitromerocyanine (SP/MRH$^+$) monolayer can also act as a "command surface" for controlling the electrical contact of redox-active proteins with a conductive support. In one example, a mixed monolayer consisting of pyridinethiol and a mercaptoalkyl nitrospiropyran (**6a**) revealed "photocommand" properties for controlling the interfacial electrochemistry of cytochrome *c* (Figure 4).[19] The photoisomerizable units give the "command" function, while the pyridinethiol monolayer functions as a promoter for electrical contact between the cytochrome *c* and the electrode.[20] The redox activity of cytochrome *c* at this interface allows the coupling of the hemoprotein to secondary enzymatic processes such as the cytochrome oxidase (COx)-activated reduction of O_2 to water (Figure 4A) or the lactate dehydrogenase (LDH)-mediated oxidation of lactate to pyruvate (Figure 4C). When the photoisomerizable groups are transformed into the positively charged protonated

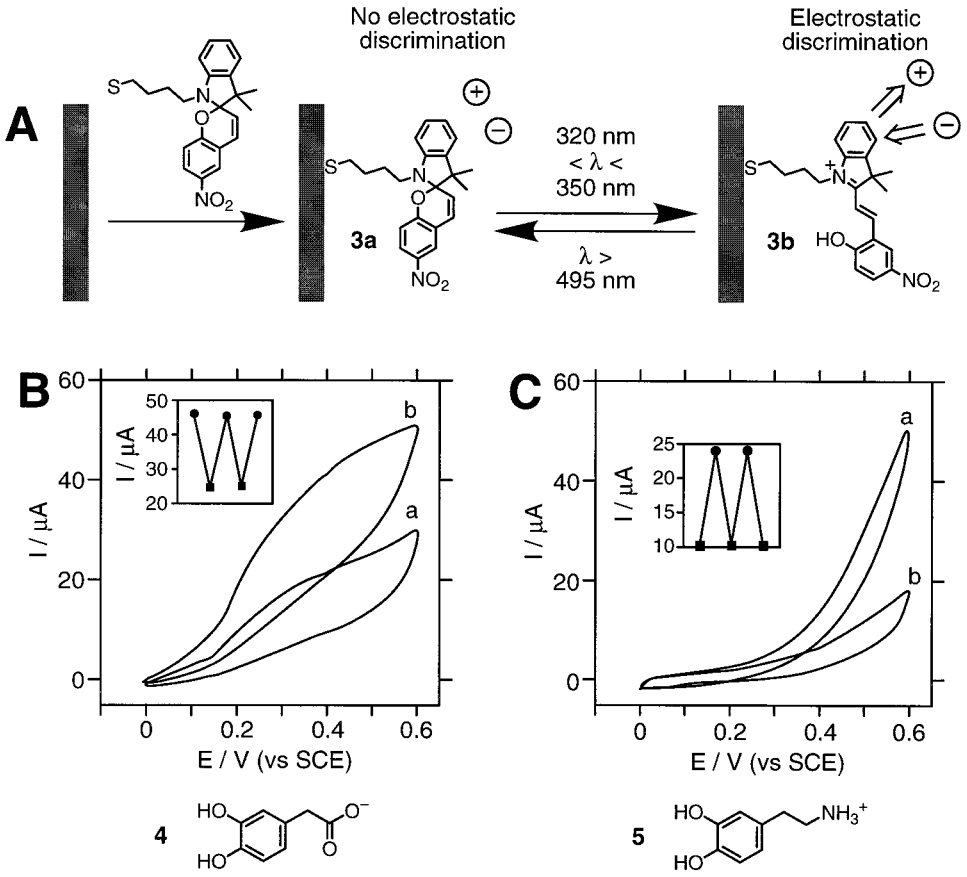

FIGURE 3. (A) Assembly and photoswitchable states of a nitrospiropyran monolayer. (B) and (C) Cyclic voltammograms of the photoisomerizable electrode in (a) the **3a** and (b) the **3b** states in the presence of (B) **4** (0.5 mM) and (C) **5** (0.5 mM). Insets: Switching of the anodic current of the system at +470 mV.

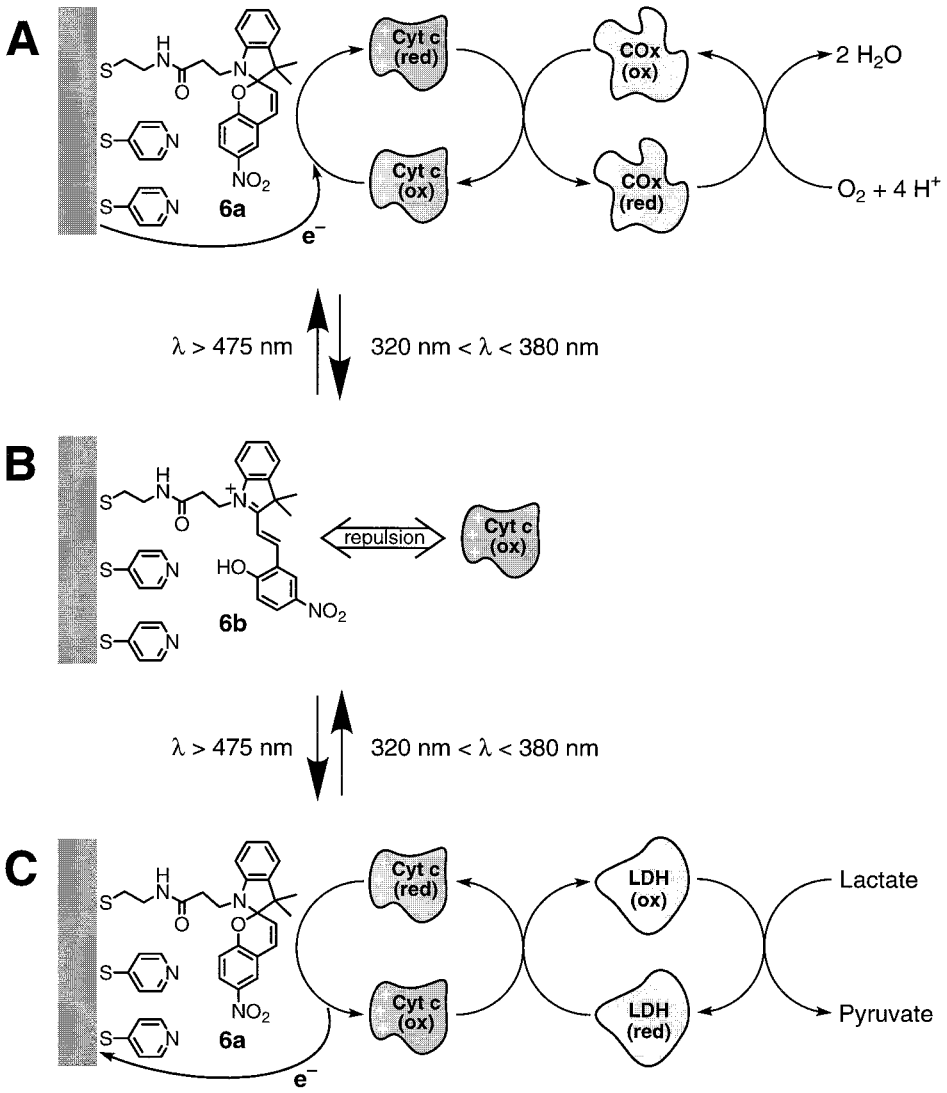

FIGURE 4. Coupling of the photoswitchable interactions between cytochrome *c* and a **6a**/pyridine mixed monolayer with (A) the reduction of O_2 by COx and (C) the oxidation of lactate by LDH. (B) When the electrode is in the cationic merocyanine state (**6b**), repulsive interactions disallow the functioning of bioelectrocatalytic processes.

merocyanine state (**6b**), the positively charged cytochrome *c* molecules are repelled from the electrode surface, and the electrical contact between the hemoprotein and the electrode is blocked (Figure 4B), also inhibiting any secondary reactions. The photoswitchable electrical contacting of cytochrome *c* with the electrode is demonstrated by cyclic voltammetry (Figure 5A), where the contacted hemoprotein yields a quasi-reversible redox wave, while the repelled protein reveals no redox activity. The coupling of the electrically activated cytochrome *c* (SP monolayer) to the COx-mediated reduction of oxygen provides a catalytic current (Figure 5B, curve a), and the deactivated cytochrome *c* (MRH^+ monolayer) inhibits the secondary biocatalytic event (Figure 5B, curve b). Upon the photochemical cycling of the monolayer between the spiropyran (SP) and merocyanine (MRH^+) states, the redox response of cytochrome *c* and the reduction of oxygen are cycled between "on" and "off" states (Figure 5A,B, insets). Related photoisomerizable command interfaces have been used to control the biocatalytic activity of negatively charged ferrocene-tethered glucose oxidase[21] and for the electrocatalytic regeneration of NAD^+ (nicotinamide adenine dinucleotide) cofactor in the presence of Ca^{2+}.[22] The isomerization of a nitrospiropyran monolayer to a protonated nitromerocyanine monolayer has also been carried out thermally,[23] and changes in monolayer charge upon protonation and deprotonation have been used to control the interfacial electrochemistry of negatively charged redox probes such as pyrroloquinoline quinone (PQQ).[24]

Photocommand interfaces may also act by the specific association of a solution-state species to one state of an isomerizable surface. A monolayer of the dinitrospiropyran **7** has thus been used for the "reversible sensing" of the anti-dinitrophenyl antibody (DNP-Ab) (Figure 6). The antibody binds strongly to **7a** (the dinitrospiropyran (SP) state of the monolayer), which acts as an antigen for DNP-Ab. The protonated dinitromerocyanine (MRH^+) state (**7b**) does not act as an antigen for the antibody, however. The changes in DNP-Ab binding as a result of the photoisomerization of the surface can be

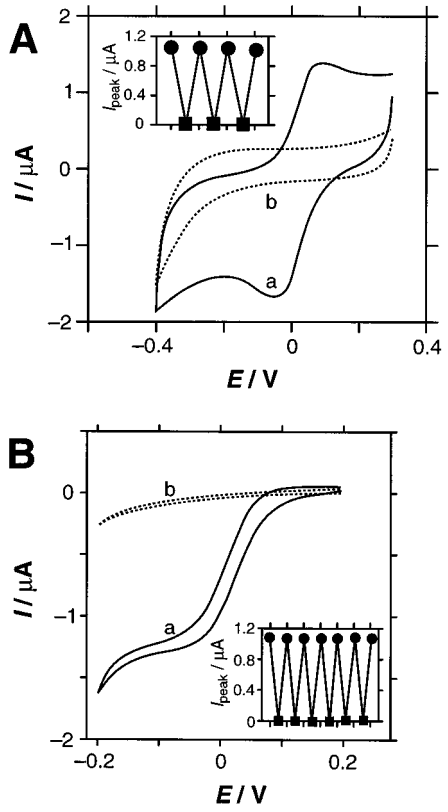

FIGURE 5. (A) Cyclic voltammetric response of cytochrome *c* (0.1 mM) at a mixed **6a/b** and pyridine monolayer-modified electrode in (a) the **6a** and (b) the **6b** states. Inset: switching behavior of the system; circles and squares represent the photoisomerizable units in the spiropyran and the merocyanine states, respectively. (B) The same system with COx (1 μM) and O_2 and in (a) the **6a** and (b) the **6b** states. Inset: Switching behavior (as for part A).

followed by cyclic voltammetry,[25] Faradaic and non-Faradaic impedance,[26] surface plasmon resonance (SPR),[27] and quartz crystal microgravimetry (QCM).[25] The SP (**7a**) surface (Figure 6A, (i)) can be used for the sensing of DNP-Ab (Figure 6A, (ii)), after which it can be photoisomerized to the MRH^+ (**7b**) state and rinsed to remove the bound antibody (Figure 6A, (iii)). Further photoisomerization back to the SP state regenerates the clean sensing interface (Figure 6A, (i)). Figure 6B shows Faradaic impedance spectra (Nyquist diagrams) of the interface in the SP and MRH^+ states (curves (i) and (iii), respectively) in the presence of $[Fe(CN)_6]^{3-/4-}$ as a redox probe. The diameter of the semicircular region of such a plot indicates the interfacial electron-transfer resistance of the electrode. Thus, the plot shows that the SP state is slightly more insulating than the MRH^+ state (which is positively charged, and so attracts the redox probe). Upon treatment of the SP interface with DNP-Ab, curve (ii) is obtained, while treatment of the MRH^+ interface gives no additional effect. We can conclude that the DNP-Ab recognizes only the SP state, and its association with the interface provides additional insulation to electron transfer. The "cyclic sensing" of DNP-Ab by the photoisomerizable monolayer electrode is demonstrated in Figure 6C. Figure 6D shows the reversible sensing of DNP-Ab by the **7** interface as transduced by surface plasmon resonance (SPR). This technique is sensitive to the changes in the thickness of the interface upon the association and dissociation of the antibody. Figure 6E shows the amperometric transduction of the photoswitchable binding and dissociation of DNP-Ab to and from the **7** monolayer. Glucose oxidase-tethered ferrocene (Fc-GOx) was used as a biocatalytic redox label that probes the interactions of the antibody with the electrode interface. Figure 6E (curve a) shows a cyclic voltammogram of the SP monolayer in the presence of Fe-GOx and glucose. The bioelectrocatalytic current indicates effective electrical contact between the enzyme and the electrode, which activates the biocatalytic oxidation of glucose. The association of DNP-Ab to the antigen monolayer inhibits electrical communication between the enzyme and the electrode as a result of the insulating protein layer that is formed on the electrode surface (curve b).

4. Mechanically Functional Surfaces

Molecular functions that are presented as mechanical take many forms, and in the most trivial case, any configurationally isomerizable molecule can be described as a machine. In this section we will consider only multicomponent systems in which a controllable noncovalent movement (e.g., a translation or rotation) takes place independent of any concomitant chemical change in the components. This mechanical change may be a consequence of a chemical isomerization, a redox change, pH, potential, or another signal.

A particularly interesting controllable mechanical change has been demonstrated for an electrode-tethered cytochrome *c* mutant.[28] The resulting tethered cytochrome *c* has a buildup of positive charge on the side facing the electrode and a relatively long distance (ca. 2 nm) from the electrode to the enzyme's active site. The distance between the redox center and the electrode may therefore be switched by the application of a potential at the electrode surface (i.e., by electrostatic forces), as shown schematically in Figure 7. At a positive potential (+0.3 V), the hemoprotein is repelled from the electrode. The tether is stretched and the protein adopts a position that places the active site distant from the electrode. The application of a negative potential (−0.3 V) reduces the heme, and an immediate step back to +0.3 V (Figure 7, step a) reveals an interfacial electron-transfer rate constant of 1.5 s^{-1} (determined by chronopotentiometry). If the negative potential is prolonged, however (Figure 7, step b), the enzyme moves toward the electrode as a consequence of electrostatic attraction. In this case, a potential step to +0.3 V (Figure 7, step c) reveals a much faster electron-transfer rate constant of 20 s^{-1}, suggesting that the enzyme's active site is significantly closer to the electrode. This figure is comparable with the electron-transfer rate constant of tethered cytochrome *c* when the active site is adjacent to the tethering site. The reverse movement of the attracted enzyme back to the extended position exhibits the same behavior.[28]

Interlocked compounds have a great potential for both mechanical and information functions. The immobiliza-

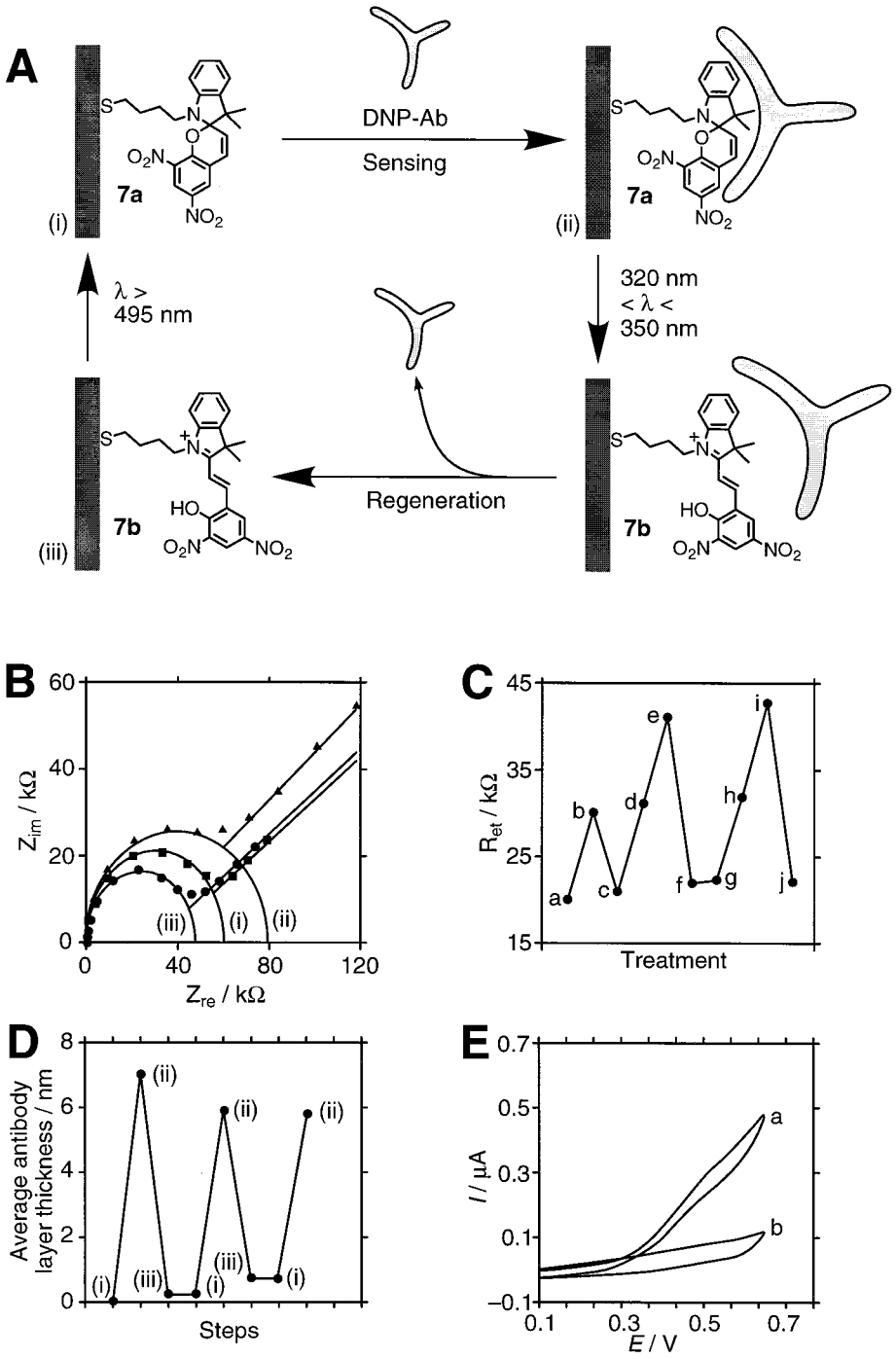

FIGURE 6. (A) A reusable sensor for DNP-Ab. (B) Faradaic impedance spectra of an electrode in configurations (i), (ii), and (iii) with $[Fe(CN)_6]^{3-/4-}$ as a redox probe. (C) Electron-transfer resistance of the photoisomerizable film moving between different states: (a, c, f, j) rinsed electrode in MRH^+ state, (b, d, h) after photoisomerization to the SP state and the addition of DNP-Ab (e, i), and (g) after addition of DNP-Ab to the electrode in MRH^+ state. (D) SPR-measured thickness of a photoisomerizable **7a** monolayer electrode upon cycling through the states (i), (ii), and (iii). (E) Cyclic voltammograms of the electrode in the presence of Fc-GOx and glucose (a) in the SP state and (b) after treatment with DNP-Ab.

tion and utilization of these structures on surfaces, although of great interest, is challenging for several reasons. Interlocked molecules tend to be large and complex, making their aligned immobilization difficult and their communication with electrodes problematic. In addition, they need enough spatial freedom to perform their mechanical function unimpeded. Despite these difficulties, however, several examples of immobilized interlocked compounds have been reported in the past year.

A catenane,[29] as well as a rotaxane,[30] has been sandwiched between conductive electrodes to give a mechanically acting electronic device. The electrically induced translocation of the internal components of the immobilized molecules results in a change in the resistance of the organic layer. Reversible translocation of the

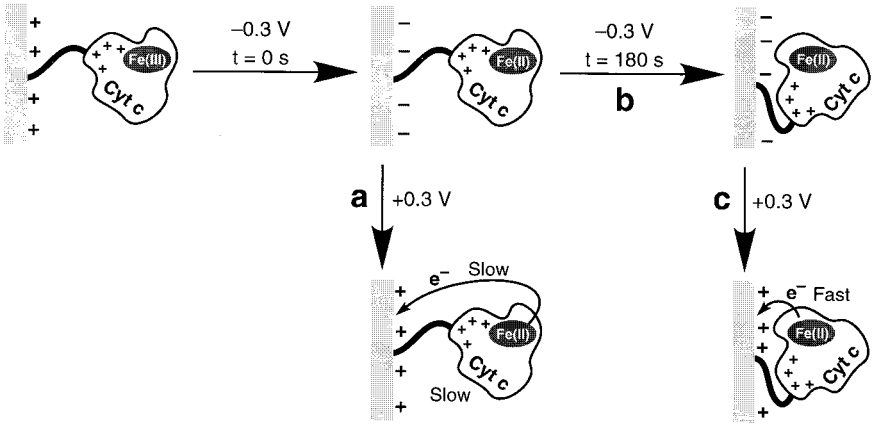

FIGURE 7. Schematic diagram of the potentiometric switching of the electrode-active site distance in a tethered cytochrome *c* mutant.

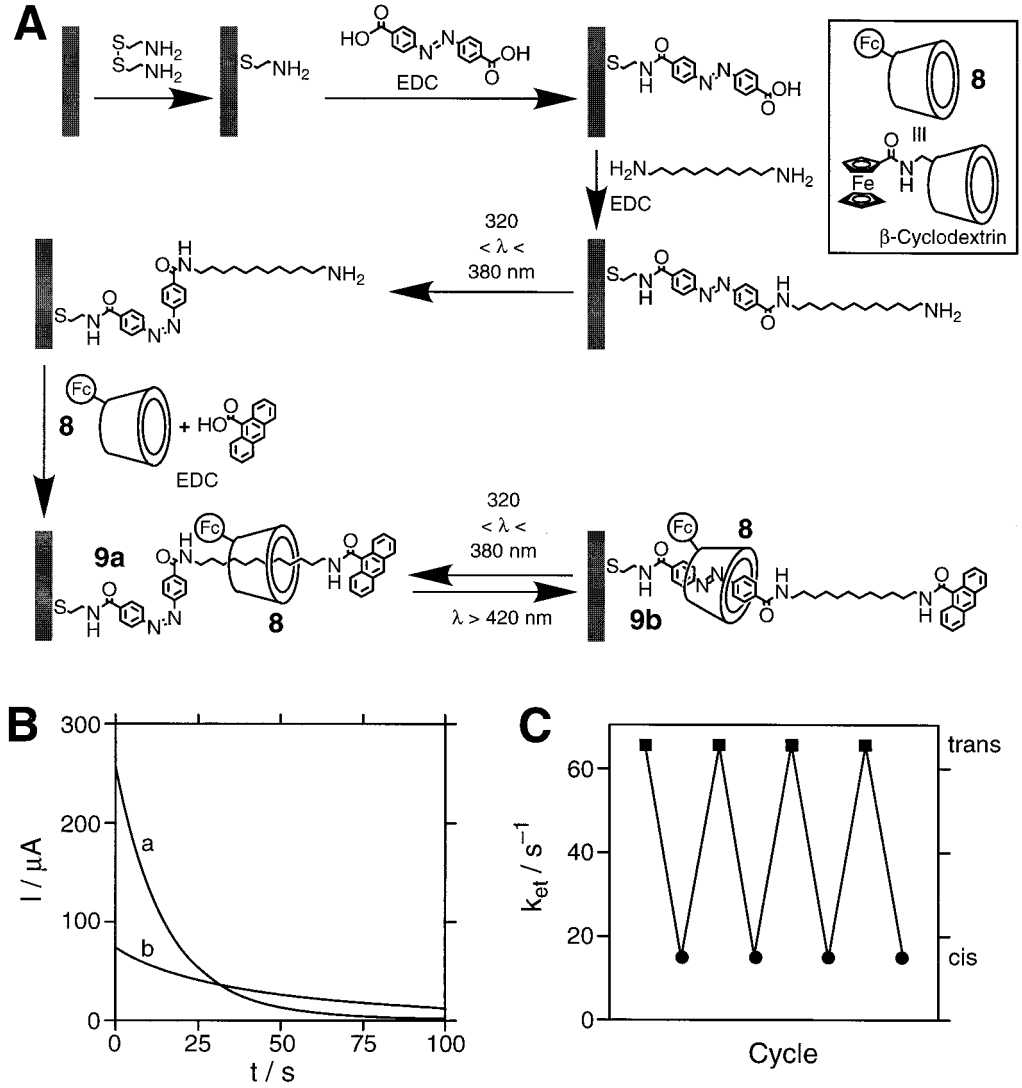

FIGURE 8. (A) Assembly and photoisomerization of a switchable rotaxane on a gold electrode. (B) The chronoamperometric response of the monolayer in (a) the *trans* state and (b) the *cis* state. (C) The electron-transfer rate constant between the electrode and the ferrocene component over four photoisomerization cycles.

molecular components allows the multiple reversible change of the electronic properties of the devices between two distinct states, labeled "ON" and "OFF". Several devices were configured together to produce AND and OR logic gates with high and low current levels separated by factors of 15 and 30, respectively (a significant enhancement over wired logic gates). The behavior of these solid-state devices can be interpreted on the basis of the redox properties of the interlocked supramolecular components in solution. The similarity of the electronic behavior of

these molecules in the solid-state devices to that in a dilute solution suggests that the device properties are determined largely by molecular properties. Thus, the devices might be scaled down to molecular dimensions without altering their fundamental properties.

A surface-bound photoswitchable rotaxane is schematically described in Figure 8A.[31] The assembly consists of a ferrocene-functionalized cyclodextrin (**8**) molecule threaded on a "string" (**9**) containing a photoisomerizable azobenzene unit and a long alkyl chain. The cyclodextrin component is prevented from dethreading by a bulky anthracene "stopper" group. When the azobenzene is in the *trans* configuration (**9b**), it is complexed by **8**, but photoisomerization to the *cis* state (**9a**) leaves complexation sterically impossible, so the **8** is translocated to the alkyl component. Back-photoisomerization to the *trans*-azobenzene structure restores the original state. The position of the cyclodextrin-tethered ferrocene unit was determined by chronoamperometry.[32] Figure 8B (curve a) shows the chronoamperometric response of the surface-bound **8**-rotaxane in the *trans* state. A fast current decay ($k_{et}^{(1)} = 65\ s^{-1}$) is observed, implying that the cyclodextrin is close to the electrode surface. Photoisomerization of the monolayer to the *cis* state results in the chronoamperometric transient shown in Figure 8B (curve b). A substantially lower electron-transfer rate constant is observed ($k_{et}^{(2)} = 15\ s^{-1}$), indicating that the cyclodextrin is more distant from the electrode surface. By cyclic photoisomerization of the monolayer between the *trans* and *cis* states, the threaded receptor can be reversibly moved between the *trans*-azobenzene site and the alkyl chain (Figure 8C).

Functionalized magnetic nanoparticles may be used for the transduction of external magnetic signals.[33] This effect was recently demonstrated by the magnetic field-switchable redox activation of magnetic particle-tethered ferrocene and *N*,*N*′-bipyridinium units (Figure 9A). The attraction of the magnetic particles to the conductive support by an external magnetic field generates a redox-active monolayer interface, whereas the shifting of the external magnet position lifts the magnetic particles from the conductive support, and their redox function is blocked. Figure 9B shows the magnetic control of the redox function of the magnetic particle-tethered ferrocene units. The magnetoswitchable redox function of the tethered redox units enables the control of biocatalyzed transformations. Figure 9C shows the magnetic control of glucose oxidation by GOx. The redox activation of tethered ferrocene by attraction to the electrode allows mediated electron transfer from GOx, and the biocatalyzed oxidation of glucose is able to proceed (Figure 9C, curve a). Lifting of the magnetic particles from the electrode by the magnetic field deactivates the tethered ferrocene units and blocks the oxidation of glucose (Figure 9C, curve b). Similarly, the bipyridinium-functionalized magnetic nanoparticles were used for the magnetically switchable reduction of nitrate to nitrite in the presence of nitrate reductase.[33]

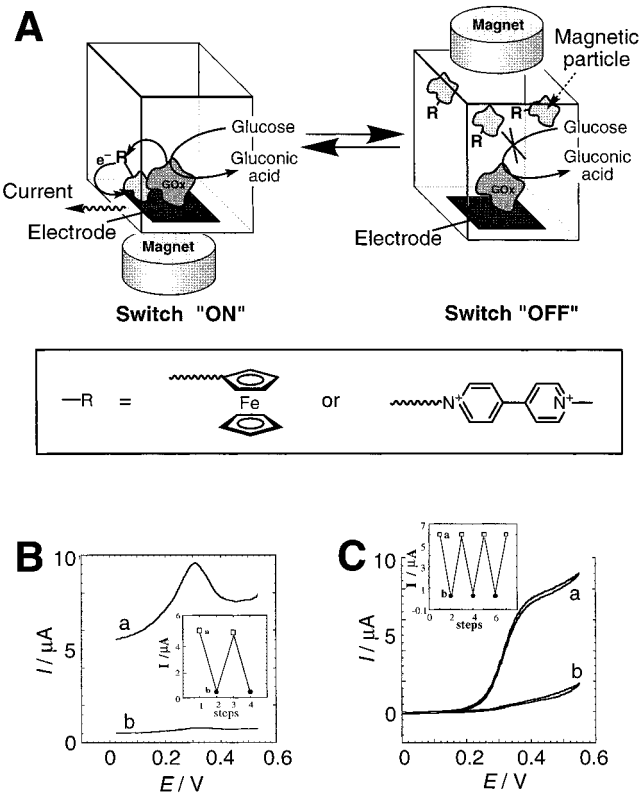

FIGURE 9. (A) Schematic diagram of the magneto-switchable oxidation of glucose. (B) Differential pulse voltammograms of ferrocene-functionalized magnetite particles with a magnet (a) below and (b) above the cell. Inset: Switching of the current. (C) Cyclic voltammograms of the system consisting of GOx, the ferrocene-functionalized magnetic particles, and glucose 8×10^{-2} M with a magnet (a) below and (b) above the cell. Inset: Switching behavior of amperometric responses of the system.

Finally, the electrochemical functions of surfaces can also be activated by the use of isomerizable polymers. Hydrogels have degrees of swelling that are functions of environmental parameters such as temperature, solvent, solutes, and electric field,[34] and the swelling of conductive polymers has been proposed for the development of "artificial muscles".[35] The incorporation of gold nanoparticles into an acrylamide hydrogel matrix leads to a composite material in which the spacing between the nanoparticles is controlled by the polymer swelling (Figure 10A).[36] The resistance of the structure depends on this interparticle spacing, and consequently, chronopotentiometric experiments can be used to transduce swell-changing stimuli. In the swollen state, nanoparticle-containing and nanoparticle-free hydrogel films have similar resistivities ($R \approx 40$ and 50 kΩ, respectively), the well-separated nanoparticles having only a small effect on conductivity. The shrinking of a nanoparticle-free gel by immersion in acetone yields an insulating film ($R \approx 170$ kΩ), as reflected by the high overpotential required to reduce a solution-state redox species (Figure 10B, curve c). This rise in resistance is attributed to a drop in porosity, isolating the electrode from the solution. A shrunken nanoparticle-containing hydrogel, however, exhibits a much lower resistance ($R \approx 1.0$ kΩ) as a consequence of the close proximity of the nanoparticles in the thinner

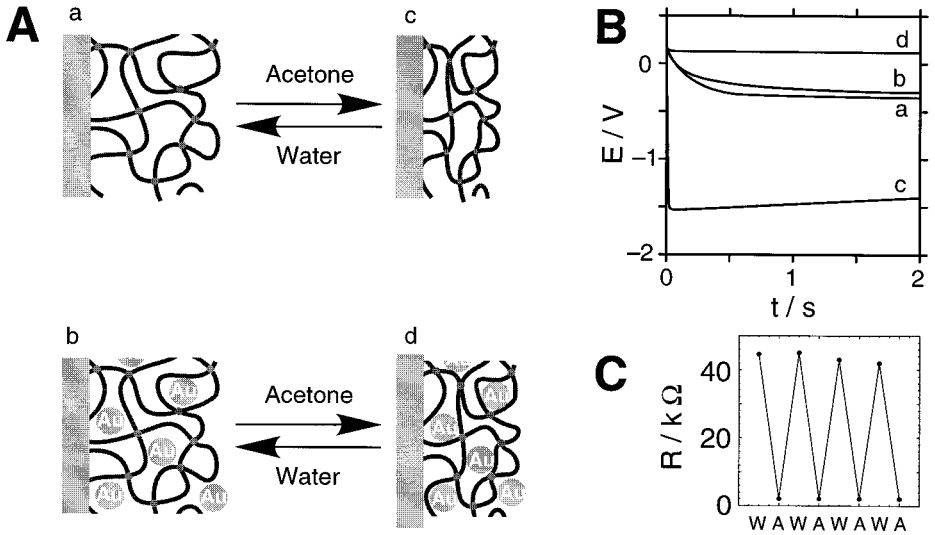

FIGURE 10. (A) Schematic diagram of the swelling and contracting of empty and nanoparticle-containing gels upon changes in solvent composition. (B) Chronopotentiometric transients of configurations a, b, c, and d. (C) Switching behavior between swollen ("W") and shrunken ("A") states.

structure facilitating conductivity. In this state, virtually no overpotential is required for the reduction of the solution-state redox label (Figure 10B, curve d). By the cyclic transformation of the composite between the swollen and shrunken states, the film can be switched between high and low resistances (Figure 10C).

5. Conclusions and Outlook

The application of surfaces is proving invaluable for the interfacing and ordering of molecular components. Methodologies for the immobilization of molecular entities on surfaces are available, and a battery of ultrasensitive spectroscopic and microscopic techniques enable the structural characterization of these systems. In this Account, we have described some simple systems for signal transduction and information storage. A phenoxynaphthacene quinone monolayer was demonstrated to exhibit an electrochemical response that can be switched on and off by the application of light and pH signals. Photoisomerizable spiropyrans were shown to behave as "command" molecules, controlling the presence of another species at an interface by either electrostatic or binding interactions. Finally, mechanical movements of immobilized species were discussed. These systems are variously composed of organic, inorganic, and biological materials, often working together to produce the desired function. It is easy to see how these simple information events can be used for the development of sensing and memory devices. More complicated electrochemical systems that operate as a function of two or more stimuli can extend this paradigm to information processing units, and the incorporation of mechanical components with these stimulus-activated molecular assemblies could ultimately lead to nanoscale devices such as signal-activated motors, pumps, and levers.[37]

Current research has shown that many surface configurations are possible, focusing on "optoelectronic" surfaces, "photocommand" surfaces, and immobilized mechanical systems. Advantage is taken of photoisomerizable units (such as phenoxynaphthacene quinones, spiropyrans, and azobenzenes) and redox units (such as bipyridinium and ferrocene derivatives) as well as biomaterials (enzymes, cofactors, antibodies, DNA), other supramolecular systems (cyclophanes, cyclodextrins, and binding motifs), and photoactive chromophores. The integration of redox-active components with conductive supports enables the electrochemical transduction of chemical events occurring on the surface. To realize the full potential of these accomplishments, future efforts must be directed at the organization of multicomponent systems with complex functions.

Recent research has accelerated the development of microscale and nanoscale functional patterns on surfaces using chemical means, stamping, scanning probe microscopies, and other techniques. The development of scanning tip methodologies such as AFM, NSOM, and ESCM allows the nanometric manipulation and addressing of molecular assemblies. Clearly, interdisciplinary research combining chemistry, physics, biology, microelectronics, and materials science will further develop the challenging topic of molecular electronics and machinery at functional surfaces.

Parts of this research are supported by the Israel Science Foundation and the U.S.-Israel Binational Foundation (BSF), contract 1998249. A.N.S. gratefully acknowledges a Valazzi-Pikovsky fellowship.

References

(1) (a) Lehn, J.-M. *Supramolecular Chemistry*; VCH Verlagsgesellschaft: Weinheim, 1995. (b) Benniston, A. C. Photo- and redox-active [2]rotaxanes and [2]catenanes. *Chem. Soc. Rev.* **1996**, 427−435. (c) Fujita, M. Self-assembly of [2]catenanes containing metals in their backbones. *Acc. Chem. Res.* **1999**, *32*, 53−61.

(2) (a) McCarty, G. S.; Weiss, P. S. Scanning probe structures of single nanostructures. *Chem. Rev.* **1999**, *99*, 1983−1990. (b) Lillehei, P. T.; Bottomley, L. A. Scanning probe microscopy. *Anal. Chem.* **2000**, *72*, 189−196.

(3) (a) Janshoff, A.; Nietzert, M.; Oberdorfer, Y.; Fuchs, H. Force spectroscopy of molecular systems—single molecule specroscopy of polymers and biomolecules. *Angew. Chem., Int. Ed.* **2000**, *39*, 3213−3237.

(4) *Organic Photochromic and Thermochromic Compounds*; Crano, J. C., Guglielmetti, R. J., Eds.; Plenum Press: New York, 1998.

(5) Amabilino, D. B.; Stoddart, J. F. Interlocked and intertwined structures and superstructures. *Chem. Rev.* **1995**, *95*, 2725−2828.

(6) (a) Willner, I.; Katz, E. Integration of layered redox-proteins and conductive supports. *Angew. Chem., Int. Ed.* **2000**, *39*, 1180−1218. (b) Armstrong, F. A.; Heezing, H. A.; Hirst, J. Reactions of complex metalloproteins studied by protein-film voltammetry. *Chem. Soc. Rev.* **1997**, *26*, 169−179. (c) Schmidt, H.-L.; Schuhmann, W. Reagentless oxidoreductase sensors. *Biosens. Bioelectron.* **1996**, *11*, 127−135.

(7) (a) Shipway, A. N.; Katz, E.; Willner, I. Nanoparticle arrays on surfaces for electronic, optical and sensoric applications. *ChemPhysChem* **2000**, *1*, 18−52. (b) Shipway, A. N.; Lahav, M.; Willner, I. Nanostructured gold colloid electrodes. *Adv. Mater.* **2000**, *12*, 993−998.

(8) (a) Zelchenok, A.; Buchholz, F.; Fisher, E.; Ratner, J.; Krongauz, V.; Anneser, H.; Bräuchle, C. Photochemistry and multiple holographical recording in polymers with photochromic phenoxynaphthacene-quinone side-groups. *J. Photochem. Photobiol. A* **1993**, *76*, 135−141. (b) Tajima, M. M.; Keat, L. E.; Matsunaga, K.; Yamashita, T.; Tokoro, M.; Inoue, H. Photochromism of 1-phenoxyanthraquinones. *J. Photochem. Photobiol. A* **1993**, *74*, 211−219. (c) Gritsan, N. P.; Klimenko, L. S. Photochromism of quinoid compounds—properties of photoinduced ana-quinones. *J. Photochem. Photobiol. A* **1993**, *70*, 103−117.

(9) (a) Doron, A.; Portnoy, M.; Lion-Dagan, M.; Katz, E.; Willner, I. Amperometric transduction and amplification of optical signals recorded by a phenoxynaphthacene quinone monolayer electrode: photochemical and pH-gated transfer. *J. Am. Chem. Soc.* **1996**, *118*, 8937−8944. (b) Doron, A.; Katz, E.; Portnoy, M.; Willner, I. An electroactive photoisomerizable monolayer electrode: a command surface for the amperometric transduction of recorded optical signals. *Angew. Chem., Int. Ed. Engl.* **1996**, *35*, 1535−1537.

(10) Cai, S.-M.; Inokuchi, H.; Fujishima, A.; Liu, Z.-F. Electrochemical behavior of azobenzene self-assembled monolayers on gold. *Langmuir* **1996**, *12*, 2843−2848.

(11) Nakashima, N.; Nakanishi, T.; Nakatani, A.; Deguchi, Y.; Murakami, H.; Sagara, T.; Irie, M. Photoswitching of a vectorial electron-transfer reaction at a diarylethene modified electrode. *Chem. Lett.* **1997**, 591−592.

(12) Liu, Z. F.; Hashimoto, K.; Fujishima, A. Photoelectrochemical information storage using an azobenzene derivative. *Nature* **1990**, *347*, 658−660.

(13) (a) Tachibana, H.; Nakamura, T.; Matsumoto, M.; Komizu, H.; Manda, E.; Niino, H.; Yabe, A.; Kawabata, Y. Photochemical switching in conductive langmuir-blodgett films. *J. Am. Chem. Soc.* **1989**, *111*, 3080−3081. (b) Tachibana, H.; Azumi, R.; Nakamura, T.; Matsumoto, M.; Kawabata, Y. New types of photochemical switching phenomena in langmuir-blodgett films. *Chem. Lett.* **1992**, 173−176. (c) Tachibana, H.; Nishio, Y.; Nakamura, T.; Matsumoto, M.; Manda, E.; Niino, H.; Yabe, A.; Kawabata, Y. Control of photochemical switching phenomena by chemical modification. *Thin Solid Films* **1992**, *210*/*211*, 293−295. (d) Tachibana, H.; Manda, E.; Azumi, R.; Nakamura, T.; Matsumoto, M.; Kawabata, Y. Multiple photochemical switching device based on Langmuir−Blodgett films. *Appl. Phys. Lett.* **1992**, *61*, 2420−2421.

(14) (a) Willner, I.; Blonder, R.; Katz, E.; Stocker, A.; Bückmann, A. F. Reconstitution of apo-glucose oxidase with a nitrospiropyran-modified FAD cofactor yields a photoswitchable biocatalyst for amperometric transduction of recorded optical signals. *J. Am. Chem. Soc.* **1996**, *118*, 5310−5311. (b) Lion-Dagan, M.; Katz, E.; Willner, I. Amperometric transduction of optical signals recorded by organized monolayers of photoisomerizable biomaterials on Au-electrodes. *J. Am. Chem. Soc.* **1994**, *116*, 7913−7914. (c) Willner, I.; Katz, E.; Willner, B.; Blonder, R.; Heleg-Shabtai, V.; Bückmann, A. F. Assembly of functionalized monolayers of redox proteins on electrode surfaces: novel bioelectronic and optobioelectronic systems. *Biosens. Bioelectron.* **1997**, *12*, 337−356. (d) Blonder, R.; Katz, E.; Willner, I.; Wray, V.; Bückmann, A. F. Application of a nitrospiropyran-FAD reconstituted glucose oxidase and charged electron mediators as optobioelectronic assemblies for the amperometric transduction of recorded optical signals: control of the 'ON'−'OFF' direction of the photoswitch. *J. Am. Chem. Soc.* **1997**, *119*, 11747−11757.

(15) (a) Lahav, M.; Ranjit, K. T.; Katz, E.; Willner, I. A beta-amino-cyclodextrin monolayer-modified Au-electrode: a command surface for the amperometric and microgravimetric transduction of optical signals recorded by a photoisomerizable bipyridinium-azobenzene dyad. *Chem. Commun.* **1997**, 259−260. (b) Lahav, M.; Ranjit, K. T.; Katz, E.; Willner, I. Photostimulated interactions of bipyridinium-azobenzene with a beta-amino-cyclodextrin monolayer-functionalized electrode: an optoelectronic assembly for the amperometric transduction of recorded optical signals. *Isr. J. Chem.* **1997**, *37*, 185−195. (c) Marx-Tibbon, S.; Ben-Dov, I.; Willner, I. Electrochemical and quartz crystal microbalance transduction of light-controlled supramolecular interactions at monolayer-functionalized electrodes. *J. Am. Chem. Soc.* **1996**, *118*, 4717−4718. (d) Ranjit, K. T.; Marx-Tibbon, S.; Ben-Dov, I.; Willner, B.; Willner, I. Light-stimulated formation and dissocation of supramolecular donor−acceptor complexes between eosin and bipyridinium azobenzenes: design of molecular electronic devices for the piezoelectric transduction of recorded optical signals. *Isr. J. Chem.* **1996**, *36*, 407−419. (e) Ranjit, K. T.; Marx-Tibbon, S.; Ben-Dov, I.; Willner, I. Optical and microgravimetric transduction of the formation of supramolecular donor−acceptor complexes between bis-pyridinium-azobenzenes and eosin in solutions and at solid interfaces. *Angew. Chem., Int. Ed. Engl.* **1997**, *36*, 147−150.

(16) (a) Lane, R. T.; Hubbard, A. T. Electrochemistry of chemisorbed molecules II. The influence of charged chemisorbed molecules on the electrode reactions of platinum complexes. *J. Phys. Chem.* **1973**, *77*, 1411−1421. (b) Takehara, K.; Ide, Y. Electrochemical properties of a gold electrode modified with a mixed monolayer. *Bioelectrochem. Bioenerg.* **1992**, *27*, 207−219.

(17) Malem, F.; Mandler, D. Self-assembled monolayers in electroanalytical chemistry−application of omega-mercapto carboxylic-acid monolayers for the electrochemical detection of dopamine in the presence of a high concentration of ascorbic acid. *Anal. Chem.* **1993**, *65*, 37−41.

(18) Doron, A.; Katz, E.; Tao, G.; Willner, I. Photochemically- chemically- and pH-controlled electrochemistry at functionalized spiropyran monolayer electrodes. *Langmuir* **1997**, *13*, 1783−1790.

(19) (a) Willner, I.; Lion-Dagan, M.; Marx-Tibbon, S.; Katz, E. Bioelectrocatalyzed amperometric transduction of recorded optical signals using monolayer-modified Au-electrodes. *J. Am. Chem. Soc.* **1995**, *117*, 6581−6592. (b) Lion-Dagan, M.; Katz, E.; Willner, I. A bifunctional monolayer electrode consisting of 4-pyridyl sulfide and photoisomerizable spiropyran. Photoswitchable electrical communication between the electrode and cytochrome c. *J. Chem. Soc., Chem. Commun.* **1994**, 2741−2742.

(20) (a) Armstrong, F. A.; Hill, H. A. O.; Walton, N. J. *Q. Rev. Biophys.* **1986**, *18*, 261−322. (b) Armstrong, F. A.; Hill, H. A. O.; Walton, N. J. Direct electrochemistry of redox proteins. *Acc. Chem. Res.* **1988**, *21*, 407−413. (c) Frew, J. E.; Hill, H. A. O. Direct and indirect electron-transfer between electrodes and redox proteins. *Eur. J. Biochem.* **1988**, *172*, 261−269.

(21) (a) Willner, I.; Doron, A.; Katz, E.; Levi, S.; Frank, A. J. Reversible associative and dissociative interactions of glucose oxidase with nitrospiropyran monolayers assembled onto Au-electrodes: Amperometric transduction of recorded optical signals. *Langmuir* **1996**, *12*, 946−954. (b) Katz, E.; Willner, B.; Willner, I. Light-controlled electron-transfer reactions at photoisomerizable monolayer electrodes by means of electrostatic interactions: active interfaces for the amperometric transduction of recorded optical signals. *Biosens. Bioelectron.* **1997**, *12*, 703−719.

(22) Katz, E.; Lion-Dagan, M.; Willner, I. Control of electrochemical processes by photoisomerizable spiropyran monolayers immobilized onto Au-electrodes: amperometric transduction of optical signals. *J. Electroanal. Chem.* **1995**, *382*, 25−31.

(23) Katz, E.; Willner, I. Thermal and photochemical control of an electrochemical process at an isomerizable spiropyran monolayer-modified Au-electrode. *Electroanalysis* **1995**, *7*, 417−419.

(24) Katz, E.; Lion-Dagan, M.; Willner, I. pH-Switched electrochemistry of pyrroloquinoline quinone at Au-electrodes modified by functionalized monolayers. *J. Electroanal. Chem.* **1996**, *408*, 107−112.

(25) (a) Willner, I.; Blonder, R.; Dagan, A. Application of photoisomerizable antigenic monolayer electrodes as reversible amperometric immunosensors. *J. Am. Chem. Soc.* **1994**, *116*, 9365−9366. (b) Blonder, R.; Levi, S.; Tao, G.; Ben-Dov, I.; Willner, I. Development of amperometric and microgravimetric immunosensors and reversible immunosensors using antigen and photoisomerizable antigen monolayer electrodes. *J. Am. Chem. Soc.* **1997**, *119*, 10467−10478.

(26) Patolsky, F.; Filanovsky, B.; Katz, E.; Willner, I. Photoswitchable antigen−antibody interactions studied by impedance spectroscopy. *J. Phys. Chem. B* **1998**, *102*, 10359−10367.

(27) Kaganer, E.; Pogreb, R.; Davidov, D.; Willner, I. Surface plasmon resonance characterization of photoswitchable antigen−antibody interactions. *Langmuir* **1999**, *15*, 3920−3923.

(28) Pardo-Yissar, V.; Katz, E.; Willner, I.; Kotlyar, A. B.; Sanders, C.; Lill, H. Biomaterial engineered electrodes for bioelectronics. *Faraday Discuss.* **2000**, *116*, 119−134.

(29) Collier, C. P.; Mattersteig, G.; Wong, E. W.; Luo, Y.; Beverly, K.; Sampaio, J.; Raymo, F. M.; Stoddart, J. F.; Heath, J. R. A [2]catenane-based solid state electronically reconfigurable switch. *Science* **2000**, *289*, 1172−1175.
(30) (a) Collier, C. P.; Wong, E. W.; Belohradsky, M.; Raymo, F. M.; Stoddart, J. F.; Kuekes, P. J.; Williams, R. S.; Heath, J. R. Electronically configurable molecular-based logic gates. *Science* **1999**, *285*, 391−394. (b) Wong, E. W.; Collier, C. P.; Behloradsky, M.; Raymo, F. M.; Stoddart, J. F.; Heath, J. R. Fabrication and transport properties of single-molecule-thick electrochemical junctions. *J. Am. Chem. Soc.* **2000**, *122*, 5831−5840.
(31) Willner, I.; Pardo-Yissar, V.; Katz, E.; Ranjit, K. T. A photoactivated 'molecular train' for optoelectronic applications: light-stimulated translocation of a beta-cyclodextrin receptor within a stoppered azobenzene-alkyl chain supramolecular monolayer assembly on a Au-electrode. *J. Electroanal. Chem.* **2001**, *497*, 172−177.
(32) Katz, E.; Willner, I. Kinetic separation of amperometric responses of composite redox-active monolayers assembled onto Au-electrodes: implications to the monolayer structure and composition. *Langmuir* **1997**, *13*, 3364−3373.
(33) Hirsch, R.; Katz, E.; Willner, I. Magnetoswitchable bioelectrocatalysis. *J. Am. Chem. Soc.* **2000**, *122*, 12053−12054.
(34) (a) Tanaka, T.; Nishio, I.; Sun, S.-T.; Uneo-Nishio, S. Collapse of gels in an electric field. *Science* **1982**, *218*, 467−469. (b) Oya, T.; Enoki, T.; Grosberg, A. Y.; Masamune, S.; Sakiyama, T.; Takeoka, Y.; Tanaka, K.; Wang, G.; Yilmaz, Y.; Feld, M. S.; Dasari, R.; Tanaka, T. Reversible molecular adsorption based on multiple-point interaction by shrinkable gels. *Science* **1999**, *286*, 1543−1545. (c) Park, T. G.; Hoffman, A. S. Synthesis and characterization of pH- and or temperature-sensitive hydrogels. *J. Appl. Polym. Sci.* **1992**, *46*, 659−671. (d) Koltz, J. H.; Holtz, J. S. W.; Munro, C. H.; Asher, S. A. Intellegent crystallized colloid arrays: novel chemical sensor materials. *Anal. Chem.* **1998**, *70*, 780−791. (e) Holtz, J. H.; Asher, S. A. Thermally switchable periodicities and diffraction from mesoscopically ordered materials. *Science* **1997**, *389*, 829−832.
(35) Sansiñena, J. M.; Olazábal, V.; Otero, T. F.; Polo da Fonseca, C. N.; De Paoli, M.-A. A solid-state artificial muscle based on polypyrrole and a solid polymeric electrolyte working in air. *Chem. Commun.* **1997**, 2217−2218.
(36) Pardo-Yissar, V.; Gabai, R.; Shipway, A. N.; Willner, I. Gold nanoparticle/hydrogel composites with solvent-switchable electronic properties. *Adv. Mater.*, in press.
(37) Lahav, M.; Durkan, C.; Gabai, R.; Katz, E.; Welland, M.; Willner, I., submitted.

AR000180H